Magnetic behavior of cosputtered Fe-Zr amorphous thin films exhibiting perpendicular magnetic anisotropy

Parmanand Sharma,* Hisamichi Kimura, and Akihisa Inoue
Institute for Materials Research, Tohoku University, Sendai 980-8577, Japan
(Received 22 August 2008; revised manuscript received 16 September 2008; published 17 October 2008)

Excellent mechanical properties of amorphous or glassy metals along with the capability to fabricate sub-50-nm patterns promise their application as a futuristic material for production of various nano- or microelectromechanical systems. In addition to their applications, these materials pose a lot of challenges in understanding their fundamental properties because of their random structure and involvement of three or more different kinds of atoms. The amorphous Fe-Zr system which is reported to exhibit superconductivity, ferromagnetism, spin glass, and antiferromagnetism is an ideal system to understand. The controversial magnetic properties of this system are still a subject of debate. In the present paper we revisited Fe-Zr system and studied their detailed magnetic properties in the temperature range of 5–330 K. Fe_xZr_{100-x} (x=63, 68, 76, 86, 92, and 93 at. %) thin films were deposited on silicon (100) substrate by a cosputtering technique. The Curie temperature (T_c) is shown to increase almost linearly with an increase in Fe concentration, but it decreases rapidly for the Fe-rich films. The films with x up to ~86 at. % have a strange shape of the hysteresis loop and are shown to exhibit perpendicular magnetic anisotropy with a stripe domain structure. Hysteresis loop shapes are correlated with the magnetic structure of the films, and provide an easy understanding of magnetic properties. It has been shown that the Fe-rich films are composed of antiferromagnetic Fe clusters which are embedded in the ferromagnetic amorphous FeZr.

DOI: 10.1103/PhysRevB.78.134414 PACS number(s): 75.70.−i, 75.50.Bb, 75.50.Kj, 75.20.En

I. INTRODUCTION

Metallic amorphous or glassy materials are gaining considerable interest from a fundamental as well as an application point of view.[1] For example these materials are used as basic building blocks for the development of nanocrystalline materials. In magnetic tunnel junctions amorphous metals are used to obtain the structural and interface perfection that are difficult to achieve with the use of single crystals because of presence of atomic steps.[2] In the production of microelectromechanical systems, amorphous or glassy metals seem to provide the best chemical and mechanical properties along with the nano- or micropatterning ability.[3,4] Single step sub-50-nm patterns have been demonstrated using the direct writing technique such as focused ion beam and mass production of large area nanopatterns using nanoimprint.[4] In order to fully realize the potential of such materials, a better knowledge of amorphous or glassy state is required, which is complicated and challenging because of disorder. The disordered structure also allows us to manipulate and tailor the average atomic configuration, which results in unreported magnetic properties even for the same alloy system.[5–7] We have mentioned above that the main hurdle in understanding these alloys is their random arrangement of atoms and in addition to this, the formation of bulk metallic glasses or amorphous alloys requires at least three or more different types of atoms in a specific composition range in order to produce the structural frustration.[1] The amorphous state can be obtained in binary alloy systems, provided the alloys are fabricated in thin film form on a substrate. Therefore thin films can provide an initial step in understanding of amorphous or glassy metals.

Since Zr can be alloyed with all the late 3*d* transition metals, Cu, Ni, Co and Fe, with a homogeneous noncrystalline phase, these metallic glasses present a unique opportunity for understanding the random structure. As a result, a considerable body of experimental and theoretical reports exists in literature. The Fe-Zr system which exhibits superconductivity, paramagnetism, ferromagnetism, and antiferromagnetism with increasing Fe content is an ideal system to understand, despite the fact that the amorphous Fe-Zr alloys are the most thoroughly studied quenched random-exchange ferromagnet in bulk[8–38] as well as in thin film[39–52] forms. Three different types of magnetic behavior are reported in the case of Fe-Zr alloys: (1) ferromagneticlike, (2) re-entrant spin glasses (RSG), and (3) spin glasses. The Fe-rich amorphous films are reported to be inhomogeneous and consist of Fe-rich spin clusters. Both ferromagnetic and antiferromagnetic natures have been reported for these spin clusters. However there are also some reports which showed absence of these clusters. Therefore the origin of magnetic properties and the existence of clusters in amorphous Fe-Zr alloys are still unclear and are a subject of debate.[53]

The wide range of compositional tunability and the nonmagnetic nature of Fe-rich FeZr make it interesting from the application point of view.[49,54–56] The insertion of nonmagnetic Fe-Zr layer in $CoFe/Al_2O_3/CoFe$ magnetic tunnel junction is effective to enhance the tunneling magnetoresistance.[54] Ferromagnetic nanometer-size dots were also fabricated in nonmagnetic amorphous Fe-Zr films using atomic force microscopy.[49] A write-once-read-many type of optical disk was also demonstrated using Fe-Zr thin films.[56] In view of the above fundamental and technical interests, here we have revisited the Fe-Zr system and systematically studied its detailed magnetic properties in a wide compositional range. In addition to clarifying the nature of magnetism, the aim is also to search for the existence of spin reorientation transition (SRT) phenomenon similar to glassy Co-Fe-Ta-B thin films.[5–7]

II. EXPERIMENT

Fe-Zr films were deposited by a dc magnetron cosputtering technique. Pure Fe and Zr-metal targets (50 mm in diameter) were used. The sputtering chamber was evacuated to a base pressure of $\sim 10^{-5}$ Pa, and high-purity argon gas (grade-1) was introduced to obtain a sputtering gas pressure of 0.2 Pa. Films were deposited on a silicon (100) substrate at substrate temperatures (T_s) ranging from room temperature (RT) to 300 °C. Separate dc power supplies were used for sputtering of both the targets. Power to the Fe target was fixed at 100 W, while power to the Zr target was varied from 0 to 100 W, to obtain different concentrations of Zr in the Fe-Zr thin films. The distance between the target and the substrate was fixed at ~150 mm. During deposition the substrate was rotated at a speed of 10 rotations per minute. All the films were deposited for the fixed time of 1 h. The film thickness obtained varied from ~275 nm (power to Zr target 10 W) to ~710 nm (power to Zr target 100 W). The compositional analysis of Fe_xZr_{100-x} films was carried out by an electron probe microanalysis technique at five different locations of each sample. The crystallographic information of the films was obtained by using a Rigaku (model: RINT-Ultima III) x-ray diffractometer (XRD). The x-ray source used was Cu $K\alpha$ radiation, and the voltage and current during measurement were 40 kV and 40 mA, respectively. During measurements, the x-ray source was fixed to an angle of 15°, and the detector was moved. For each step (step width=0.05°), the diffracted intensity was recorded for a fixed time of 5 s. Resistivity was measured in the temperature range of 78–450 K by using a commercial resistivity measurement system (ResiTest 8300, Toyo Corp. Japan) configured for Van der Pauw method. Detailed magnetic measurements in the temperature range of 5–330 K were performed using a Quantum Design superconducting magnetometer (MPMS 5S). The magnetic-field direction was in-plane in all the magnetic measurements, unless it is specified as out-of-plane. In zero-field-cooled (ZFC) measurements, the sample was cooled to 5 K from 300 K in zero magnetic field and after that a constant magnetic field of 20 Oe was applied and magnetization was measured with increasing temperature (in the case of hysteresis loops, magnetization was measured by changing the magnetic field at constant temperature). For field-cooled (FC) measurements, the sample was cooled in a constant magnetic field of 20 Oe from 300 to 5 K and the magnetization was measured with increasing temperature under the same magnetic field (in the case of FC hysteresis loops, magnetization was measured at a constant temperature by varying the magnetic field). The temperature dependence of thermoremanent magnetization (TRM) was measured after cooling the sample in the magnetic field of 20 Oe from room temperature (above Curie temperature) down to 5 K and then reducing the magnetic field to zero.

III. RESULTS AND DISCUSSION

A. Structural characterization

It was observed that the Fe concentration in the films decreases almost linearly with an increase in power to the Zr target [Fig. 1(a)]. XRD curves for $Fe_xZr_{(100-x)}$, x =63–93 at. %, thin films deposited at RT are shown in Fig. 1(b). A broad peak characteristic of an amorphous state can be noticed for x=63–92 at. %. It is observed that the maximum peak intensity decreases and the peak position shifts toward higher angles with an increase in Fe concentration in the films. It is hard to comment on the basis of the peak intensity, but in the present case all the x-ray measurements were performed under similar conditions (such as same acceleration current and voltage, fixed time of measurement, same size of the samples, etc.), therefore we can say that the decrease in peak intensity is because of a reduction in film thickness with increasing concentration of Fe in the film, and is consistent with our sputtering conditions. A further increase in Fe content to x=93 at. % results in the appearance of a sharp peak at $2\theta \sim 44.3°$, which is superimposed on a broad peak [Fig. 1(b)]. The analysis of this diffraction pattern revealed that the Fe-Zr thin films with Fe content of 93 at. % consist of nanocrystals of α-Fe precipitated in the remaining amorphous phase. For x=86 at. %, films were also deposited on heated substrates with a maximum substrate temperature (T_s) of ~300 °C. We did not observe any appreciable difference in the XRD patterns of the films deposited at elevated T_s and the films deposited at room temperatures.

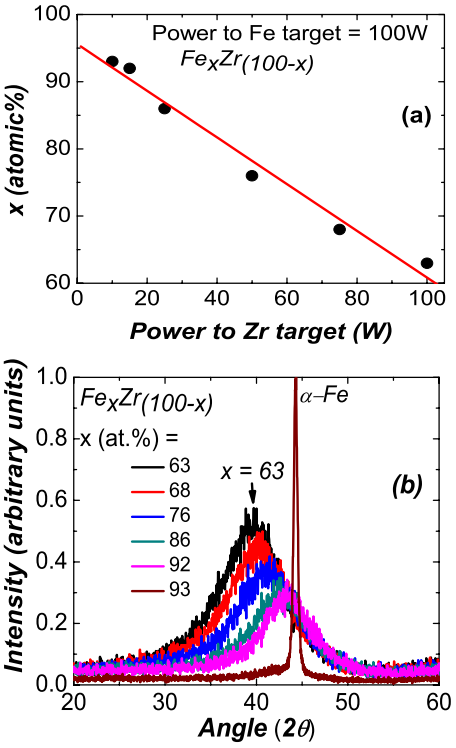

FIG. 1. (Color online) (a) Dependence of Fe concentration in Fe-Zr thin films with the power applied to Zr target during cosputtering of Fe (100 W) and Zr. (b) XRD patterns of $Fe_xZr_{(100-x)}$ (x =63, 68, 76, 86, 92, and 93 at. %) thin films showing amorphous nature up to 92 at. % Fe in the films. All the XRD curves are normalized by the intensity of α-Fe peak for x=93 at. %.

B. Electrical resistivity

High electrical resistivity is also reported in the case of amorphous alloys.[57] Figure 2 shows the electrical resistivity

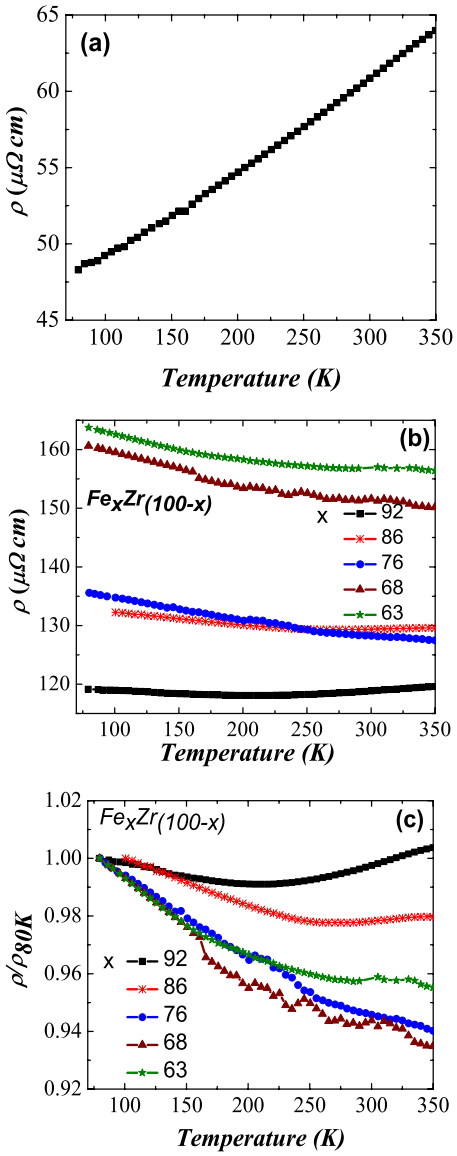

FIG. 2. (Color online) Temperature dependence of resistivity (a) for nanocrystalline plus amorphous thin films (x=93 at. %), (b) for amorphous thin films, and (c) for amorphous films normalized by the resistivity at 80 K. The figure shows low resistivity and positive TCR for nanocrystalline plus amorphous, and high resistivity along with negative TCR for amorphous Fe-Zr thin films.

measured in the temperature range of 80–350 K for $Fe_xZr_{(100-x)}$ (x=63–93 at. %) thin films. At low temperatures (~80 K), resistivity of amorphous $Fe_xZr_{(100-x)}$ (x=63 at. %) thin film is ~3.4 times higher than the amorphous plus nanocrystalline $Fe_xZr_{(100-x)}$ (x=93 at. %) thin film [Figs. 2(a) and 2(b)]. Moreover, it is ~2.6 times higher at room temperature. For amorphous films, the absolute value of resistivity at a particular temperature depends on Fe concentration in the film. In general, it decreases with an increase in Fe concentration for the entire measured temperature range [Fig. 2(b)], except for the films having Fe content of 76 and 86 at. %. A crossover in resistivity at ~250 K is observed, which results in a slightly higher value of resistivity at room temperature for x=86 at. % as compared to x=76 at. % [Fig. 2(b)]. Amorphous films also exhibit a weak negative temperature coefficient of resistivity (TCR). Such a temperature variation is in contrast to the majority of metallic alloys. However, in the case of amorphous or glassy metals both positive and negative TCR are found. It is known that alloys composed of atoms with d electrons have high resistivity and often exhibit negative TCR. As expected for normal metallic systems, nanocrystalline plus amorphous $Fe_xZr_{(100-x)}$ (x=93 at. %) thin film has a positive TCR [Fig. 2(a)].

On careful examination of Fig. 2(c), a minimum in resistivity (T_m) can be noticed in the case of Fe-rich films. Fukamichi *et al.*[40] reported that the resistivity minimum is at the magnetic Curie temperature (T_c). However, Stobiecki *et al.*[43] did not observe any definitive correlation with T_c. For Fe concentration less than 25 at. % they observed that the resistivity decreases with an increase in temperature even up to 400 K. For Fe concentration above 75 at. %, resistivity exhibits a minimum which shifts toward lower temperatures. Our results are in good agreement with these reported results. The minimum in resistivity is also observed in many other amorphous or glassy magnetic systems.[58]

C. Magnetic characterization

1. Curie temperature (T_c)

Figure 3(a) shows the temperature-dependent magnetization [$M(T)$] curves measured under in-plane magnetic fields of 1000 Oe for x=63–86 at. % and 5000 Oe for x=92 and 93 at. % Fe in the Fe-Zr films. Under these intensities of magnetic fields, the film magnetization was saturated or close to saturation. All the $M(T)$ curves have a similar shape, however, the magnetization at room temperature is almost zero for all the films except x=93 at. %. Moreover the x=93 at. % film exhibits a small decrease in magnetization around 260 K. All these observations point out that the Curie temperature for amorphous Fe-Zr thin films is lower than room temperature. In the case of x=93 at. % film, a significantly high value of magnetization at room temperature results from the α-Fe precipitates, whereas the small decrease in the magnetization at ~260 K is due to the T_c of the remaining amorphous phase. These magnetic measurements are consistent with our XRD measurement shown in Fig. 1(b). In order to obtain a value of T_c, the curves shown in Fig. 3(a) were differentiated, and the minimum in the curve was considered as the value of T_c.[47] The variation in T_c with Fe concentration in the films is shown in Fig. 3(b). The T_c is below room temperature for all the films, and a maximum occurs at the Fe concentration between 76 and 86 at. %. The increase in T_c with an increase in Fe concentration in the films is normal in the case of ferromagnetic materials; however, the opposite trend observed in Fig. 3(b) for the Fe-rich films is unusual. A similar trend in the variation of T_c with Fe concentration has also been reported for ribbons and thin films of amorphous Fe-Zr alloys.[11,40,43] The observed decrease in T_c at higher concentrations of Fe was explained on the basis of antiferromagnetic exchange interactions that can emerge in Fe-rich amorphous alloys. However the maximum in T_c was reported to occur at a Fe concentration of

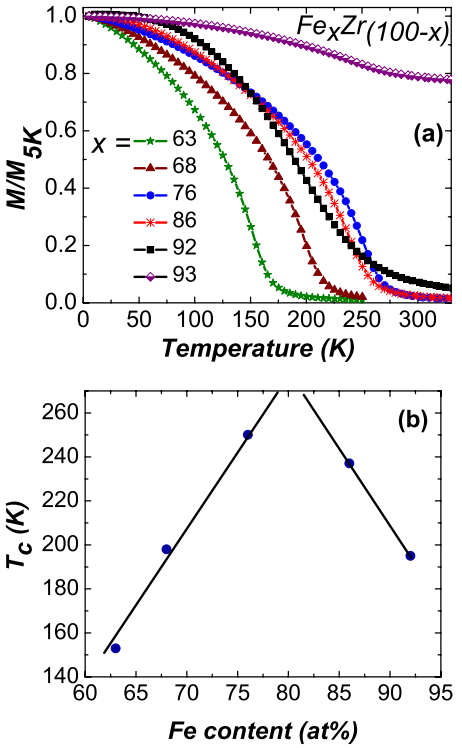

FIG. 3. (Color online) (a) Temperature-dependent magnetization curves for $Fe_xZr_{(100-x)}$ (x=63, 68, 76, 86, 92, and 93 at. %) thin films measured in in-plane saturating magnetic field, and (b) variation in Curie temperature (T_c) with Fe concentration for amorphous Fe-Zr thin films, showing a rapid decrease in T_c for Fe-rich thin films.

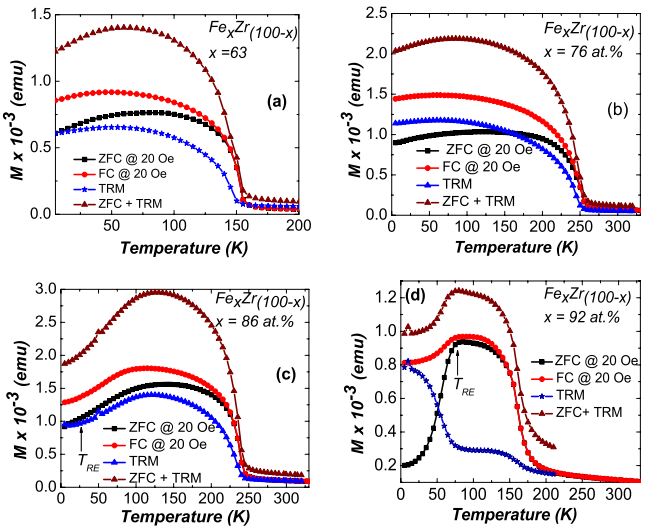

FIG. 4. (Color online) ZFC, FC, TRM, and ZFC+TRM curves measured under an in-plane magnetic field of 20 Oe for amorphous $Fe_xZr_{(100-x)}$ [x=(a) 63, (b) 76, (c) 86, and (d) 92 at. %] thin films.

~85 at. % which is slightly higher as compared to the present study. The reason for this deviation seems to be the presence of stress in the films because deposition of the films at heated substrate resulted in a significant increase in T_c. For example, T_c of the $Fe_xZr_{(100-x)}$ (x=86) film increases from 237 K for the film deposited at RT to 280 K for the film deposited at T_s=300 °C.

It is worth discussing the correlation between T_c and temperature-dependent resistivity minimum (T_m) observed in Fig. 2 for Fe-rich thin films. For x=86 at. %, T_m is 280 K and T_c is 237 K. For x=92 at. % T_m is 210 K and T_c is 195 K. As T_m is broad in this compositional range, the uncertainty in determination is large. Therefore we can say that both the T_m and T_c are close to each other for Fe-rich Fe-Zr amorphous thin films. These observations suggest that the resistivity minimum around T_c is related to the magnetic behavior. There were attempts to explain this behavior by considering additional contribution from spin-dependent electron-magnon scattering to the electrical resistivity in addition to the structural disorder scattering.[32]

2. Type of magnetism—Ferromagnetic, spin glass, re-entrant?

Three different types of magnetic behavior have been reported in the case of Fe-Zr alloys: (1) ferromagneticlike alloys characterized by the T_c, (2) RSG characterized by two transition temperatures, T_c denoting a transition from paramagnetic to ferromagnetic state and T_f from ferromagnetic to spin-glass (SG) state, and (3) spin glasses, where only one transition from paramagnetic to spin-glass state occurs at T_g. The most useful measurements to infer the intrinsic magnetic behavior are ZFC/FC and TRM measurements.[59–62] Figure 4 shows the ZFC and FC curves along with TRM measured by applying an in-plane magnetic field of 20 Oe for amorphous $Fe_xZr_{(100-x)}$ (x=63, 76, 86, and 92 at. %) thin films. It can be noticed that both the ZFC and FC curves depart from each other right from the T_c. In amorphous (frustrated) systems the deviation between ZFC and FC is governed by spin dynamics and is usually observed below the onset of freezing-in of the magnetic moments. The cusp of ZFC may be governed by local anisotropy fields acting on the magnetic moments. The spins may be frozen in directions governed by their local anisotropy or by the external magnetic field if the system is cooled down from a temperature higher than freezing temperature (T_f) in zero or nonzero fields, respectively, leading to a difference in ZFC and FC magnetization.

In the case of spin glass, the difference in FC and ZFC magnetization is expected to coincide with TRM, i.e.,[60–62]

$$M_{\mathrm{FC}}(T,H) = \mathrm{TRM}(T) + M_{\mathrm{ZFC}}(T) - 0, \qquad (1)$$

where 0 represents the zero level of magnetization. The deviation from this behavior may arise from anisotropy. As evident from Fig. 4, there is a significant difference in the FC and (ZFC+TRM) magnetizations, suggesting that the amorphous Fe-Zr thin films studied in the present case are not pure spin glasses. Another characteristic feature observed in the case of spin glasses is the continuous decay of TRM with increasing temperature up to T_f, which is again absent in the present case.[62] The sharp rise and the saturation in TRM with decreasing temperature are characteristic of a ferromagnetic phase. However, after saturation in TRM below T_c, an insignificant decrease can be noticed with a further decrease in temperature for the films having Fe contents up to 76 at. % [Figs. 4(a) and 4(b)]. This low temperature decrease in TRM becomes significant with a further increase in Fe concentra-

tion [Fig. 4(c)] in the films. The most Fe-rich film (x =92 at. %) exhibits two clear steps in TRM, one at T_c and another around 75 K (named as T_{RE}). This type of behavior was observed in the case of re-entrant magnets.

In the reported literature it has been established that the Fe-rich Fe-Zr amorphous alloys have two magnetic transitions: a paramagnetic to ferromagnetic at T_c, and from ferromagnetic to re-entrant (RE) state at low temperatures.[53] The RE state is proposed to be a mixed state in which long-range ferromagnetic order coexists with the spin-glass order, but the exact nature of ferromagnetic and spin-glass order still remains a highly controversial issue, and found four model descriptions.[53] The first approach considers the magnetic microstructure consisting of antiferromagnetic Fe spin clusters, and the ferromagnetic Fe-Zr matrix in which these spin clusters freeze randomly below re-entrant transition (T_{RE}).[11,14,17,23] The second model[13] depicts the spin system for $T \leq T_c$ as comprising of an infinite three-dimensional ferromagnetic matrix and finite ferromagnetic spin clusters with noncollinear spin structure embedded in a spin-canted ferromagnetic matrix, which freeze in random directions for $T \leq T_{RE}$. According to the third model,[18] the amorphous Fe-Zr alloy is a wandering axis ferromagnet in which noncollinear magnetic moments are ferromagnetically correlated but the local magnetic axis changes throughout the sample. The fourth model[34] mentions that the spin system is composed of ferromagnetically correlated longitudinal (z-axis) spin component, and strongly fluctuating transverse component (xy). As the temperature is lowered below T_c transverse spin components cooperatively freeze in random orientations in the xy plane at $T \equiv T_{RE} \leq T_{xy}$ and coexist with collinear ferromagnetic order along z direction. In Sec. III C 3 we will try to understand a model that is applicable for the present case.

3. Bloch law

It is well known that the homogeneous glassy or amorphous ferromagnets follow the Bloch's law[63,64]

$$M(T) = M(0)[1 - BT^{3/2}], \tag{2}$$

where $M(0)$ is the saturation magnetization at 0 K, and B is the characteristic constant of spin wave, and is related to the spin wave stiffness constant D as

$$B = 2.612 \frac{1}{M(0)} \left(\frac{k_b}{4\pi D} \right)^{3/2}. \tag{3}$$

Figure 5(a) shows the reduced magnetization $M(T)/M(0)$ as a function of $T^{3/2}$ for all the amorphous Fe-Zr thin films. It can be seen that the $Fe_xZr_{(1-x)}$ (x=63, 68, and 76) obey Bloch's law in the temperature range up to $\sim 0.5T_c$. From the slope of the straight line, we obtained $B = 3.31 \times 10^{-4}$, 2.15×10^{-4}, and 1.48×10^{-4} for x=63, 68, and 76, respectively. These values are 2 orders of magnitude larger than the crystalline Fe ($B = 3.4 \times 10^{-6}$ $K^{-3/2}$). The difference in the values of B between the crystalline and the glassy ferromagnets originates from the structural differences. It has been found that in an amorphous alloy the disordered atomic structure leads to an increase in spin wave density of states at low excitation energies. Consequently, the value of B is larger in the amorphous state compared to the crystalline one.[63,64] Thus, the high value of B and the dominance of Bloch law in a very large temperature range are the characteristics of a homogeneous glassy or amorphous ferromagnet. However, the Fe-rich films (x=86 and 92) do not follow Bloch's law and are not simple ferromagnetic. Kaul[13] found that the x =90 alloy behaves like a weak itinerant ferromagnet in that it exhibits a T^2 decrease in magnetization with temperature. However, Beck and Kronmuller[65] showed that the T^2 dependence gives a way to a $T^{3/2}$ law if the measurements are made in the field >0.37 T. It is to be noted that in the present case the measurements were made in the magnetic field of 0.5 T.

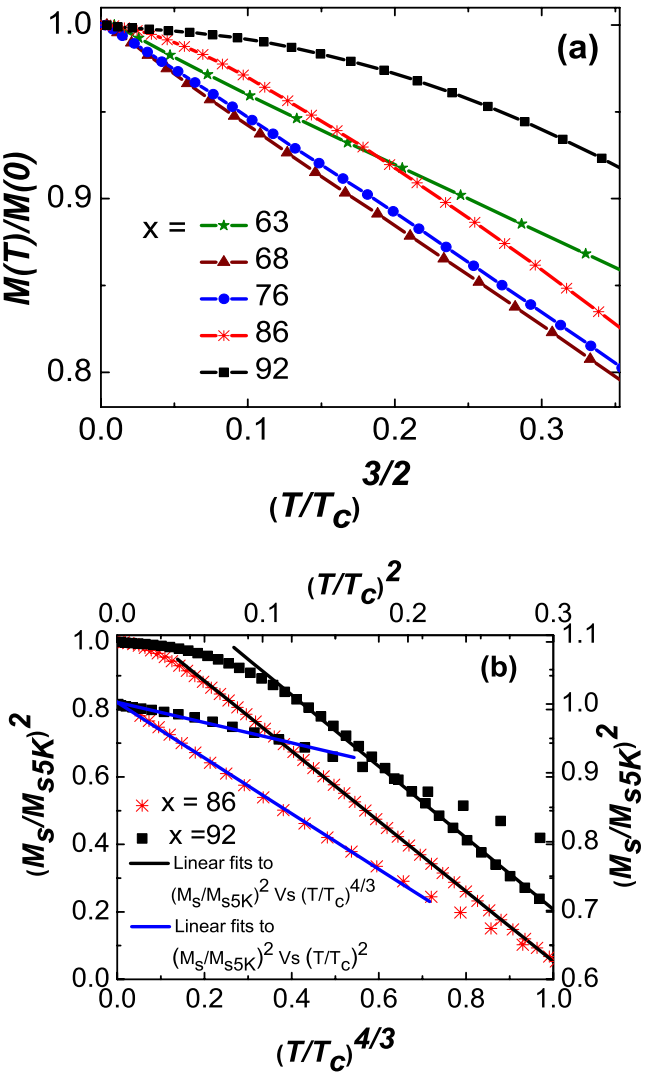

FIG. 5. (Color online) (a) Reduced magnetization $M(T)/M(0)$ as a function of $T^{3/2}$ (fitting to Bloch's law) for amorphous $Fe_xZr_{(100-x)}$ (x=63, 68, 76, 86, and 92 at. %) thin films, showing excellent linear fitting up to x=76 at. %, and (b) $[M/M_{5\ K}]^2$ vs $(T/T_c)^{4/3}$ and $(T/T_c)^2$ for x=86 and 92 at. %, showing linear fit to T^2 at low temperatures and $T^{4/3}$ below T_c in a large temperature range indicating weak itinerant electron ferromagnetism for Fe-rich films.

Takahashi[66] reported a new spin fluctuation theory for weak itinerant electron ferromagnets, in which quantum spin

fluctuations (zero-point spin fluctuations) are considered. According to this theory, $M(T)^2$ follows the $T^{4/3}$ dependence in a wide temperature range below T_c except for very low temperatures, at which T^2 dependence is observed. Figure 5(b) shows the $[M/M_{5\ K}(T)]^2$ vs $(T/T_c)^{4/3}$ and $(T/T_c)^2$ for Fe-rich amorphous $Fe_xZr_{(1-x)}$ ($x=86$ and 92) thin films. It can be noticed that the square of magnetization shows a T^2 dependence at lower temperature and $T^{4/3}$ dependence in the wide temperature range below T_c. Based on the above results and the discussion it can be inferred that the amorphous Fe-Zr thin films with Fe contents up to 76 at. % are ferromagnetic, whereas the Fe-rich films exhibit weak itinerant electron ferromagnetism.

4. Magnetic hysteresis—existence of perpendicular magnetic anisotropy

Figure 6(a) shows the hysteresis loops measured at 5 K for the $Fe_xZr_{(100-x)}$ ($x=63$, 68, 76, 86, and 92) thin films. A strange shape of the hysteresis loops for $x<86$ at. % in the films can be observed. Noticeable characteristics of these hysteresis loops are low values of reduced remanence (M_r/M_s: M_r remanence magnetization, and M_s saturation magnetization) and coercivity (H_c), and a linear increase in magnetization from M_r to M_s. To our knowledge, this type of hysteresis loop shape has not been reported in the case of amorphous Fe-Zr alloys. However, in other materials such types of hysteresis loops have been observed, and named as "transcritical hysteresis loops."[5–7,67] The magnetization behavior of a transcritical type hysteresis loop is governed by the two processes: (1) alignment of in-plane magnetization at low fields by domain-wall motion, and (2) rotation of perpendicular magnetization in the film plane at higher fields. We also examined other systems which showed similar hysteresis loop shapes at room temperature by magnetic force microscopy (MFM).[6,7] In all the cases, well-defined stripe domain patterns were observed. The bright and dark contrasts of stripe domain patterns in MFM image are due to magnetization canted upward or downward out of the film plane. Another reason for bright and dark contrasts in MFM image may be due to an oscillating magnetization with an in-plane component, and an out-of-plane component that periodically changes sign. The volume fraction of in-plane magnetization and out-of-plane magnetization can be qualitatively inferred from the hysteresis loop. A careful examination of hysteresis loops shown in Fig. 6 for amorphous Fe-Zr thin films revealed that only 15–20% of the saturation magnetization of the films reverses suddenly at low magnetic fields. Majority of magnetization reverses its direction linearly with magnetic field. These observations suggest that the $Fe_xZr_{(100-x)}$ ($x<86$ at. %) thin films exhibit perpendicular magnetic anisotropy with a stripe domain structure below RT. The existence of perpendicular magnetic anisotropy was also confirmed from the hysteresis loops measured by applying the magnetic field in the out-of-plane of the films. As an example, the hysteresis loops near origin for the $Fe_xZr_{(100-x)}$ ($x=86$ at. %) thin film measured at 100 K in out-of-plane and in-plane directions are shown in Fig. 6(b). It can be noticed that the value of H_c (~110 Oe) is higher in out-of-plane direction compared to in-plane (~20 Oe). The hysteresis loops in out-of-plane direction exhibit almost linear variation in magnetization with field and the magnetization saturates over 1.5 T [inset of Fig. 6(b)]. This behavior is because of strong demagnetization effects, and is also observed in other systems.[6,7]

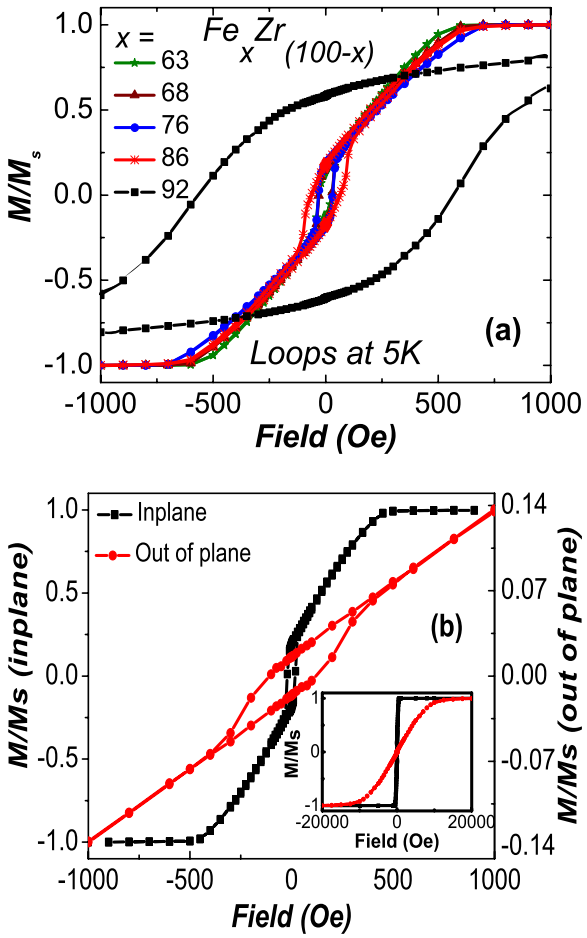

FIG. 6. (Color online) (a) In-plane hysteresis loops measured at 5 K for amorphous $Fe_xZr_{(100-x)}$ ($x=63$, 68, 76, 86, and 92 at. %) thin films, and (b) zoom in of in-plane and out-of-plane hysteresis loops near origin for amorphous $Fe_xZr_{(100-x)}$ ($x=86$ at. %) thin films at 100 K. The inset shows the complete hysteresis loops; a linear variation in magnetization with field in out-of-plane direction is because of strong demagnetization effects.

Amorphous or glassy alloys are expected to behave isotropic with respect to their structure and properties. However, thin films prepared by evaporation or sputtering sometimes show a columnar structure that can lead to magnetic anisotropy in the films. The column orientation in vapor-deposited films is related to the vapor incidences and can be explained in terms of self-shadowing. However, in our experimental capabilities, we could not detect any columnar growth structure in these films. In amorphous or glassy alloys, unlike crystalline materials, symmetry is absent and principally each atom constitutes a structural unit. These materials do not exhibit long-range order such as crystals, but short-range order which extends over a range of neighbor shells of atoms up to a distance of about 1 nm is well known. The existence of short-range order seems to be responsible

for the perpendicular magnetic anisotropy in amorphous Fe-Zr thin films.

5. Spin clusters

Another interesting feature which can be noticed from Fig. 6(a) is a rapid increase in coercivity for Fe-rich films. In order to understand it, we measured hysteresis loops at different temperatures. Figure 7(a) shows the hysteresis loops measured at different temperatures for Fe-Zr thin films with Fe content of 63 at. %. It can be noticed that the transcritical hysteresis loop shape persists almost up to T_c, however, before going to the paramagnetic state, hysteresis loop shape becomes normal. We observed a similar hysteresis behavior for Fe contents up to 86 at. % in the films, however, this is different for x=92 at. % [Fig. 7(b)]. Variation in H_c with temperature for all the Fe-Zr thin films is shown in Fig. 7(c). It can be noticed that for Fe concentrations up to 76 at. % in the films, H_c decreases almost linearly with an increase in temperature. A rapid increase in H_c at low temperatures is noticed in the case of films having Fe concentrations ≥86 at. % and can be fitted to the following equation [Fig. 6(a); solid lines are the fit]:[23]

$$H_c = H_c(\Theta)e^{-\beta T}. \tag{4}$$

On careful examination of hysteresis loops shown in Figs. 7(a) and 7(b), one can also notice a difference in high-field behavior. The magnetization does not saturate even in the field of 5 kOe and exhibits noticeable high-field susceptibility in the case of Fe-rich films, whereas for a lower concentration of Fe in the films, magnetization attains saturation in the field of ~0.5 kOe. Similar to the present observations, an exponential temperature variation of H_c and finite high-field susceptibility were also reported in the literature for amorphous Fe-rich Fe-Zr alloys.[22,23] The origin of this behavior was suggested as the freezing-in of the Fe-rich regions or spin clusters at low temperatures, which act as pinning centers for the domain-wall motion. Existence and magnetism (ferro- or antiferro-) of these clusters were strongly debated (as we mentioned above that magnetic behavior of Fe-Zr alloys gained four model descriptions).

Based on our understanding of the reported literature and the present magnetic data, it seems that the Fe-rich Fe-Zr films are composed of antiferromagnetic Fe-rich spin clusters, and the ferromagnetic Fe-Zr matrix in which these spin clusters freezes randomly below re-entrant transition (T_{RE}). Rapid increase in H_c at lower temperatures is due to freezing of these clusters, which act as pinning centers for the domain-wall motion. We have mentioned that the initial magnetization (low field) is governed by the rapid alignment of in-plane magnetization by domain-wall motion. If these nonmagnetic frozen Fe clusters really exist, they should affect the shape of the hysteresis loop at low fields. A careful examination of the hysteresis loops measured at 5 K reveals that the magnetization change from negative to positive or vice versa is very rapid (straight) at lower concentrations of Fe (<86 at. %) in the films, whereas it becomes slower (rounding of hysteresis loop) in the Fe-rich films (x >86 at. %) [Fig. 6(a)]. This can be easily understood on the basis of hindrance in domain-wall motion produced by the

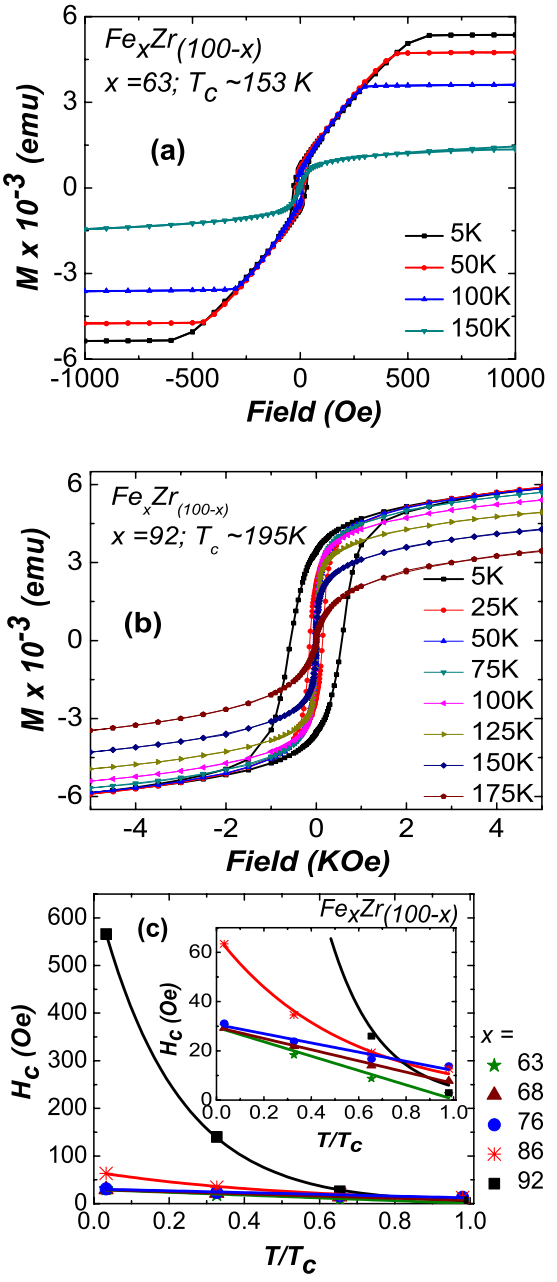

FIG. 7. (Color online) (a) In-plane hysteresis loops measured at different temperatures for (a) lowest concentration of Fe (x =63 at. %), (b) highest concentration of Fe (x=92 at. %) in amorphous Fe-Zr thin films, and (c) variation in H_c with temperature for amorphous Fe$_x$Zr$_{(100-x)}$ (x=63, 68, 76, 86, and 92 at. %) thin films, showing almost linear behavior up to x=76 at. % (as shown in inset) and exponential behavior for Fe-rich films (x>76 at. %).

frozen nonmagnetic Fe clusters. Moreover, if these clusters really freeze below T_{RE}, we should also see the changes in the hysteresis loop shape below and above T_{RE}. In fact we can observe such changes very clearly in the case of the Fe-Zr films with x=86 at. %, and the results are shown in Fig. 8. The rounding of the hysteresis loop shape near the origin observed at 5 K tends to vanish in the hysteresis loops measured at 50 K, and finally it disappears above T_{RE}

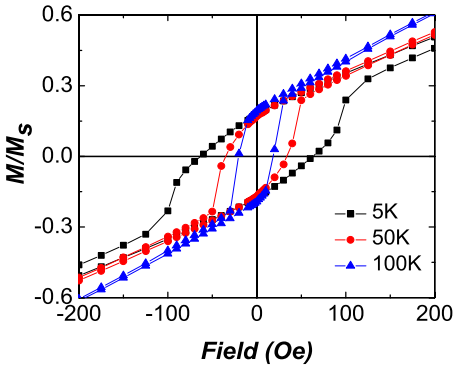

FIG. 8. (Color online) Blowup of hysteresis loops near origin measured at different temperatures for Fe concentration of 86 at. % in amorphous Fe-Zr films, showing rounding of hysteresis loop shape near origin observed at 5 K disappeared at 100 K.

~75 K (loop at 100 K). This is consistent with unfreezing of Fe clusters.

The antiferromagnetic nature of Fe clusters can be inferred from the zero-field-cooled and field-cooled hysteresis measurements. The exchange interaction between ferromagnetic and antiferromagnetic materials has often been observed to lead to a phenomenon called "exchange bias." In the hysteresis loop, it manifests itself as a shift of field-cooled hysteresis loop toward the negative field axis (negative x axis) and an increase in loop width.[68] Figure 9 shows the zero-field-cooled and field-cooled hysteresis loops measured at 5 K for the Fe-Zr thin films with a Fe concentration of 63 and 92 at. %. Presence of exchange bias for Fe-rich [Fig. 9(b)] and absence of exchange bias for lower concentration Fe [Fig. 9(a)] in Fe-Zr thin films can be noticed.

Recently we have observed the SRT phenomenon from in-plane single-domain-like state to out-of-plane multidomain with increasing temperature and film thickness. Amorphous structure along with stress in the film was shown to govern this phenomenon.[5–7] Although Fe-Zr thin films are also in an amorphous state, we do not observe SRT in Fe-Zr thin films investigated in the temperature range of 5–330 K. It should be noted that the shape of the hysteresis loops observed in the case of amorphous Fe-Zr thin films is similar to glassy Co-Fe-Ta-B thin films after SRT temperature.[5–7] The absence of SRT in amorphous Fe-Zr thin films may be because of inhomogeneous structure or the low SRT temperature below 5 K.

IV. CONCLUSIONS

Magnetic and electrical properties of $Fe_xZr_{(100-x)}$ (x=63, 68, 76, 86, 92, and 93 at. %) thin films deposited by a cosputtering technique were studied in the temperature range of 5–330 K. The films are amorphous up to Fe contents of 92 at. %. A slight increase in Fe concentration (~93 at. %) results in the precipitation of α-Fe nanocrystals in the amorphous phase. Completely amorphous films exhibit higher electrical resistivity compared to crystalline films. The amorphous films showed weak negative TCR in contrast to the nanocrystalline film which exhibited positive

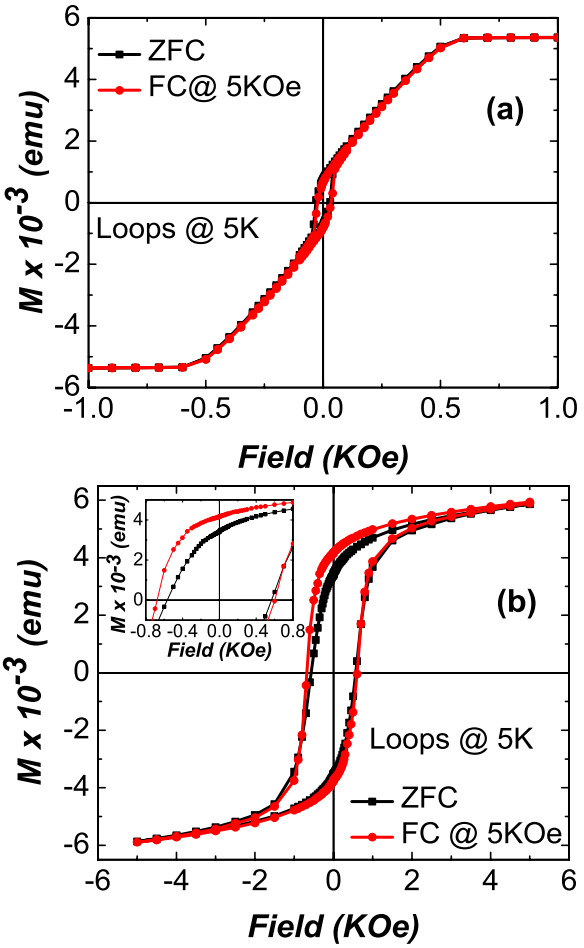

FIG. 9. (Color online) (a) ZFC and FC hysteresis loops measured at 5 K for (a) lowest concentration of Fe (x=63 at. %) and (b) highest concentration of Fe (x=92 at. %) in amorphous Fe-Zr thin films. Figure shows presence of exchange bias for Fe-rich and absence of exchange bias for low concentration of Fe in amorphous Fe-Zr thin films.

TCR. Resistivity minimum was observed in Fe-rich films, but it does not have any correlation with the Curie temperature. The T_c of amorphous Fe-Zr thin films increases with an increase in Fe contraction up to ~80 at. % and further increase in Fe content results in a decrease in T_c. $Fe_xZr_{(100-x)}$ films are magnetically homogeneous for $x<86$ at. % and exhibit perpendicular magnetic anisotropy with a stripe domain type of magnetic structure. For these films H_c varies linearly with temperature. The Fe-rich films are inhomogeneous, and are made up of Fe-rich antiferromagnetic spin cluster embedded in the ferromagnetic Fe-Zr amorphous matrix. An exponential variation of H_c with temperature was observed. The Fe-rich films also exhibit weak itinerant electron ferromagnetism. The existence of special "transcritical type" hysteresis loops (perpendicular magnetic anisotropy) for Fe-Zr thin films allows an easy understanding of magnetic structure of highly controversial Fe-rich Fe-Zr amorphous thin films. Featureless surface topography with high concentration of nonmagnetic Fe at room temperature in the films can be useful for fabrication of magnetic storage and magnetic nanostructures by local crystallization.

*Corresponding author; sharmap@imr.tohoku.ac.jp

[1] A. Inoue, Acta Mater. **48**, 279 (2000).
[2] D. Djayaprawira, K. Tsunekawa, M. Nagai, H. Maehara, S. Yamagata, N. Watanabe, S. Yuasa, Y. Suziki, and K. Ando, Appl. Phys. Lett. **86**, 092502 (2005).
[3] M. Ishida, H. Takeda, N. Nishiyama, K. Kita, Y. Shimizu, Y. Saotome, and A. Inoue, Mater. Sci. Eng., A **449-451**, 149 (2007).
[4] P. Sharma, N. Kaushik, H. Kimura, Y. Saotome, and A. Inoue, Nanotechnology **18**, 035302 (2007).
[5] P. Sharma, H. Kimura, and A. Inoue, J. Appl. Phys. **101**, 09N502 (2007).
[6] P. Sharma, H. Kimura, and A. Inoue, J. Appl. Phys. **100**, 083902 (2006).
[7] P. Sharma, H. Kimura, A. Inoue, E. Arenholz, and J.-H. Guo, Phys. Rev. B **73**, 052401 (2006).
[8] S. Ohnuma, K. Shirakawa, M. Nose, and T. Masumoto, IEEE Trans. Magn. **16**, 1129 (1980).
[9] K. Shirakawa, S. Ohnuma, M. Nose, and T. Masumoto, IEEE Trans. Magn. **16**, 910 (1980).
[10] H. Hiroyoshi and K. Fukamichi, Phys. Lett. **85A**, 242 (1981).
[11] H. Hiroyoshi and K. Fukamichi, J. Appl. Phys. **53**, 2226 (1982).
[12] Y. Obi, L. C. Wang, R. Motsay, and D. G. Onn, J. Appl. Phys. **53**, 2304 (1982).
[13] S. N. Kaul, Phys. Rev. B **27**, 6923 (1983).
[14] D. A. Read, T. Moyo, and G. C. Hallam, J. Magn. Magn. Mater. **44**, 279 (1984).
[15] R. W. Cochrane, M. Trudeau, and J. O. Strom-Olsen, J. Appl. Phys. **57**, 3207 (1985).
[16] J. O. Strom-Olsen, Z. Altounian, R. W. Cochrane, and A. B. Kaiser, Phys. Rev. B **31**, 6116 (1985).
[17] N. Saito, H. Hiroyoshi, K. Fukamichi, and Y. Nakagawa, J. Phys. F: Met. Phys. **16**, 911 (1986).
[18] D. H. Ryan, J. M. D. Coey, E. Batalla, Z. Altounian, and J. O. Strom-Olsen, Phys. Rev. B **35**, 8630 (1987).
[19] K. Nahm, W. H. Kettler, M. Rosenberg, and R. Wernhardt, J. Phys. F: Met. Phys. **17**, 2085 (1987).
[20] G. K. Nicolaides, W. Gong, G. C. Hadjpanayis, and K. V. Rao, Mater. Sci. Eng. **99**, 69 (1988).
[21] M. Ghafari, W. Keune, R. A. Brand, R. K. Day, and J. B. Dunlop, Mater. Sci. Eng. **99**, 65 (1988).
[22] D. A. Read, T. Moyo, S. Jassim, R. A. Dunlap, and G. C. Hallam, J. Magn. Magn. Mater. **82**, 87 (1989).
[23] D. A. Read, G. C. Hallam, and M. Chirwa, J. Magn. Magn. Mater. **82**, 83 (1989).
[24] H. Ma, H. P. Kunkel, and G. Williams, J. Phys.: Condens. Matter **3**, 5563 (1991).
[25] H. Ma, Z. Wang, H. P. Kunkel, and G. Williams, J. Phys.: Condens. Matter **4**, 1993 (1992).
[26] G. K. Nicolaides and K. V. Rao, J. Magn. Magn. Mater. **125**, 195 (1993).
[27] L. F. Barquin, J. C. Gomez Sal, P. D. Babu, and S. N. Kaul, J. Magn. Magn. Mater. **133**, 82 (1993).
[28] L. F. Kiss, T. Kemeny, I. Vincze, and L. Granasy, J. Magn. Magn. Mater. **135**, 161 (1994).
[29] T. Moyo, J. Magn. Magn. Mater. **154**, 201 (1996).
[30] P. Gorria, I. Orue, M. L. Fernandez-Gubieda, F. Plazaola, N. Zabala, and J. M. Barandiarn, J. Magn. Magn. Mater. **157-158**, 203 (1996).
[31] T. Moyo, J. Phys.: Condens. Matter **8**, 8915 (1996).
[32] V. Srinivas, Phys. Status Solidi B **207**, 233 (1998).
[33] L. Karlsson and R. L. McGreevy, J. Phys.: Condens. Matter **11**, 9249 (1999).
[34] D. H. Ryan, J. M. Cadogan, and J. van Lierop, Phys. Rev. B **61**, 6816 (2000).
[35] A. R. Wildes, N. Cowlam, S. Al-Heniti, L. F. Kiss, and T. Kemeny, Physica B **276-278**, 712 (2000).
[36] L. F. Barquin, J. C. Gomez Sal, P. Gorria, J. S. Garitaonandia, and J. M. Barandiaran, Eur. Phys. J. B **35**, 3 (2003).
[37] A. R. Wildes, J. R. Stewart, N. Cowlam, S. Al-Heniti, L. F. Kiss, and T. Kemeny, J. Phys.: Condens. Matter **15**, 675 (2003).
[38] M. Dikeakos, Z. Altounian, and M. Fradkin, Phys. Rev. B **70**, 024209 (2004).
[39] K. H. J. Buschow and P. H. Smit, J. Magn. Magn. Mater. **23**, 85 (1981).
[40] K. Fukamichi, R. J. Gambino, and T. R. McGuire, J. Appl. Phys. **53**, 2310 (1982).
[41] C. L. Chien, K. M. Unruh, A. Levy, S. H. Liou, J. P. Stokes, R. J. Gambino, and K. Fukamichi, J. Appl. Phys. **53**, 2307 (1982).
[42] K. M. Unruh and C. L. Chien, Phys. Rev. B **30**, 4968 (1984).
[43] T. Stobiecki, M. Przybyslki, and J. Sokulski, J. Magn. Magn. Mater. **41**, 199 (1984).
[44] H. U. Krebs, D. J. Webb, and A. F. Marshall, Phys. Rev. B **35**, 5392 (1987).
[45] M. El Hafidi, G. Chouteau, O. Bethoux, and A. Sadoc, J. Magn. Magn. Mater. **81**, 1 (1989).
[46] Byung-II Cho, W. Win, A. Manthiram, and R. M. Walser, IEEE Trans. Magn. **30**, 4443 (1994).
[47] F. J. Castano, T. Stobiecki, M. R. J. Gibbs, and H. J. Blythe, J. Phys.: Condens. Matter **9**, 1609 (1997).
[48] M. Ding, F. Zeng, and F. Pan, Nucl. Instrum. Methods Phys. Res. B **170**, 79 (2000).
[49] S. Tomino, H. Saito, and S. Ishio, J. Magn. Magn. Mater. **212**, 69 (2000).
[50] M. Gupta and A. Gupta, Phys. Status Solidi C **1**, 3211 (2004).
[51] L. Smardz, K. Smardz, and H. Niedoba, Phys. Status Solidi B **243**, 227 (2006).
[52] A. Iljinas, D. Milcius, and J. Dudonis, Vacuum **81**, 1213 (2007).
[53] S. N. Kaul, Curr. Sci. **88**, 78 (2005).
[54] K. Jun, J. H. Lee, K. H. Shin, K. Rhie, and B. C. Lee, J. Magn. Magn. Mater. **286**, 158 (2005).
[55] A. Liebig, P. T. Korelis, H. Lidbaum, G. Andersson, K. Leifer, and B. Hjorvarsson, Phys. Rev. B **75**, 214202 (2007).
[56] Byung-II Cho, Songnam-Shi, Hyeong-Chang Hong, and Ahsan-shi, United States Patent No. 6,066,381 (23 May 2000).
[57] E. Blasberg, D. Korng, and H. Pfeifle, J. Phys. F: Met. Phys. **9**, 1821 (1979).
[58] B. Shen, H. Guo, H. Gong, W. Zhan, and J. Zhao, J. Appl. Phys. **81**, 4661 (1997).
[59] B. K. Srivastava, A. Krishnamurthy, V. Ghose, J. Mattsson, and P. Nordblad, J. Magn. Magn. Mater. **132**, 124 (1994).
[60] E. Lahderanta, K. Eftimova, R. Laiho, H. A. Kanani, and J. G. Booth, J. Magn. Magn. Mater. **130**, 23 (1994).
[61] R. Laiho, K. G. Lisunov, E. Lahderanta, P. Petrenko, J. Salminen, V. N. Stamov, and V. S. Zakhvalinskii, J. Phys.: Condens. Matter **12**, 5751 (2000).
[62] R. Mathieu, P. Jonsson, D. N. H. Nam, and P. Nordblad, Phys. Rev. B **63**, 092401 (2001).
[63] C. L. Chien and R. Hasegawa, Phys. Rev. B **16**, 2115 (1977).

[64] T. Kaneyoshi, *Introduction to Amorphous Magnets* (World Scientific, Singapore, 1992).
[65] W. Beck and H. Kronmuller, Phys. Status Solidi B **132**, 449 (1985).
[66] Y. Takahashi, J. Phys.: Condens. Matter **13**, 6323 (2001).
[67] M. Coisson, F. Celegato, E. Olivetti, P. Tiberto, F. Vinai, and M. Baricco, J. Appl. Phys. **104**, 033902 (2008).
[68] M. Gruyters, Phys. Rev. Lett. **95**, 077204 (2005).